AIP | Applied Physics Letters

Single-crystalline metal filament-based resistive switching in a nitrogen-doped carbon film containing conical nanopores

Fei Zhuge, Jun Li, Hao Chen, Jun Wang, Liqiang Zhu, Baoru Bian, Bing Fu, Qin Wang, Le Li, Ruobing Pan, Lingyan Liang, Hongliang Zhang, Hongtao Cao, Hong Zhang, Zhicheng Li, Junhua Gao, and Kang Li

Citation: Applied Physics Letters **106**, 083104 (2015); doi: 10.1063/1.4913588
View online: http://dx.doi.org/10.1063/1.4913588
View Table of Contents: http://scitation.aip.org/content/aip/journal/apl/106/8?ver=pdfcov
Published by the AIP Publishing

Single-crystalline metal filament-based resistive switching in a nitrogen-doped carbon film containing conical nanopores

Fei Zhuge,[1,a)] Jun Li,[1,2] Hao Chen,[1,3] Jun Wang,[4] Liqiang Zhu,[1] Baoru Bian,[1] Bing Fu,[1] Qin Wang,[4] Le Li,[4] Ruobing Pan,[1] Lingyan Liang,[1] Hongliang Zhang,[1] Hongtao Cao,[1,a)] Hong Zhang,[3] Zhicheng Li,[3] Junhua Gao,[1] and Kang Li[1]

[1]*Ningbo Institute of Materials Technology and Engineering, Chinese Academy of Sciences, Ningbo 315201, China*

[2]*Nano Science and Technology Institute, University of Science and Technology of China, Suzhou 215123, China*

[3]*School of Materials Science and Engineering, Central South University, Changsha 410083, China*

[4]*Department of Microelectronic Science and Engineering, Faculty of Science, Ningbo University, Ningbo 315211, China*

(Received 28 January 2015; accepted 11 February 2015; published online 24 February 2015)

In this letter, we report on the resistive switching originating from the rupture/rejuvenation of single-crystalline Cu filaments in a nitrogen-doped porous carbon-based memristive device Cu/$CN_{0.15}$/Pt. Cu filaments are confined in conical nanopores in $CN_{0.15}$ thin films. Dislocations exist in the Cu filaments, resulting in obvious crystal lattice distortions. The Cu/$CN_{0.15}$/Pt device shows outstanding high temperature retention performance for both ON and OFF states, indicating that it is promising for resistance memory applications. Furthermore, continuous RESET (ON-to-OFF switching) and SET (OFF-to-ON switching) processes could be realized indicating the adaptive learning ability of Cu/$CN_{0.15}$/Pt, which has potential applications in synaptic devices. © *2015 AIP Publishing LLC*. [http://dx.doi.org/10.1063/1.4913588]

Resistive switching (RS) between a high resistance state (HRS or OFF state) and a low resistance state (LRS or ON state) arising from the electrically induced formation/rupture of metal (Cu, Ag, etc.) filaments has been reported in two-terminal memristive devices with various switching media,[1,2] such as oxides,[3–9] chalcogenides,[10–13] silicon,[14] carbon,[15–19] and polymers.[20] An electroforming process is always necessary for the initial formation of metal filaments, switching the devices ON. A RESET process can switch the devices back to the OFF state. A subsequent SET process again switches the devices to the ON state. In those cases, the electroformed metal filament is composed of continuous or discontinuous metal nano-grains.[21]

Our previous study reported electroforming-free RS in a nanoporous $CN_{0.15}$ thin film-based memristive device with ready-made metal filaments.[22] In this letter, we show that the metal filaments confined in conical nanopores have a single-crystalline structure with lattice defects, such as dislocations. The corresponding memristive device shows outstanding high temperature retention performance for both ON and OFF states. Furthermore, continuous RESET and SET processes have been realized in such device, indicating that it can potentially be used as an electronic synapse device.

60 nm thick amorphous N-doped carbon thin films were deposited on Pt/Ti/SiO_2/Si substrates by DC magnetron sputtering of a graphite target under pure N_2 ambient at room temperature (RT). The composition of as-sputtered films was determined to be $CN_{0.25}$ by X-ray photoelectron spectroscopy (XPS). The film thickness was reduced to ~25 nm after annealing at 600 °C in Ar ambient for 10 min. The composition of annealed samples was determined to be $CN_{0.15}$ by XPS. The N content loss and the film thickness reduction result from the formation of volatile products such as N_2 and C_2N_2.[22] The structure of the carbon films was checked by cross-sectional transmission electron microscopy (TEM). The TEM specimen was prepared by focus ion beam (FIB) system using a finely focused beam of gallium ions. The surface morphology and leakage current were investigated by conducting atomic force microscopy (CAFM). Cu/$CN_{0.15}$/Pt memristive devices were fabricated by depositing 50 nm thick Cu top electrodes of 100 μm in diameter onto $CN_{0.15}$ films at RT using electron-beam evaporation technique with an *in situ* metal shadow mask. To prevent Cu from oxidizing, a 20 nm thick Au protection layer was deposited on the Cu electrodes by electron-beam evaporation. Electrical characteristics of Cu/$CN_{0.15}$/Pt were measured at RT in air using a Keithley 4200 semiconductor parameter analyzer. During the measurement in voltage sweeping and pulse modes, the bias voltage was applied to the top electrode (Cu) while the bottom electrode (Pt) was grounded.

CAFM was used to simultaneously detect the surface morphology and leakage current of $CN_{0.25}$ and $CN_{0.15}$ films (Fig. 1). $CN_{0.25}$ has a relatively smooth and dense surface without any pinhole (Fig. 1(a)) whereas $CN_{0.15}$ contains numerous pores several tens of nanometers in size (Fig. 1(c)). Both films are highly resistive since no clear leakage current was observed in the corresponding CAFM images (Figs. 1(a) and 1(c)). For facilitating the CAFM investigation, a 50 nm thick Cu layer was deposited on both films followed by dissolving the Cu layer in $Fe(NO_3)_3$ aqueous solution. After removing the Cu layer, while $CN_{0.25}$ remains highly resistive (Fig. 1(b)), a large amount of bright spots were observed in CAFM images for $CN_{0.15}$ (Fig. 1(d)),

a)Authors to whom correspondence should be addressed. Electronic addresses: zhugefei@nimte.ac.cn and h_cao@nimte.ac.cn.

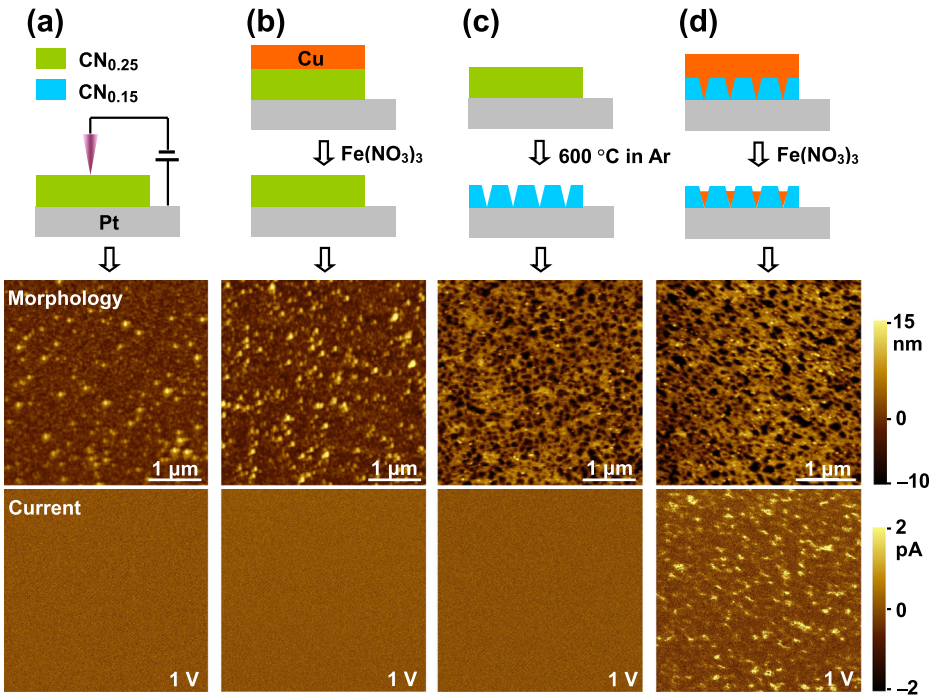

FIG. 1. CAFM images of (a), (b) as-sputtered and (c), (d) annealed N-doped carbon thin films. For facilitating the structural investigation of $CN_{0.25}$ and $CN_{0.15}$, a 50 nm thick Cu layer was deposited on both films followed by dissolving the Cu layers in $Fe(NO_3)_3$ aqueous solution. Schematic illustrations of the CAFM measurement configuration, chemical and thermal treatment processes, and film structures are also shown.

indicating that $CN_{0.15}$ is locally conductive. We see from Fig. 1(d) that the high current spots and the pores match each other in position. Then, the local high conductivity for $CN_{0.15}$ can be explained by the formation of Cu nanofilaments in the through-pores during the Cu evaporation process. Only part of the Cu filament near the film surface was dissolved in the $Fe(NO_3)_3$ aqueous solution and the rest remained. It is important to note that the size of each high current spot is smaller than that of the corresponding pore, implying that the pores are mostly likely of a conical shape with two openings, the wide opening (base) located at the film surface and the narrow one (tip) at the film/substrate (Pt) interface, as schematically illustrated in Fig. 1(c).

Direct evidence for the formation of conical nanopores in $CN_{0.15}$ films was provided by cross-sectional TEM (Figs. 2(a)–2(c)). A cone-shaped through-pore was clearly observed in Fig. 2(a), with the base size of ~30 nm. The tip size was estimated to be less than 2 nm from the corresponding high resolution TEM (HRTEM) image (Fig. 2(b)). The generation of volatile products in N-containing carbon films upon annealing at elevated temperatures should account for the formation of conical nanopores.[22] A nascent (incomplete) conical pore was also observed in Fig. 2(a), which is located close to the film surface. Thus, we can deduce that the pores are initially generated near the film surface and then extended towards the film/substrate interface. Figure 2(d) schematically illustrates the formation process of conical nanopores in N-doped carbon thin films.

As shown in Fig. 3(a), the pristine Cu/$CN_{0.15}$/Pt presents a resistance as low as ~40 Ω. The initial low resistance state can be RESET to an OFF state by applying a sufficient negative voltage. The normal *I*–*V* curves (see Fig. 3(b)) show a typical nonvolatile bipolar RS performance, i.e., the OFF state (or ON state) can be SET (or RESET) to an ON state (or OFF state) by applying a sufficient positive (or negative) voltage. The Cu/$CN_{0.15}$/Pt devices show good endurance and retention properties at RT.[22] Furthermore, the devices exhibit outstanding thermal stability. As shown in Fig. 3(c), the devices can keep their ON or OFF state stable upon heat treatment at 120 °C in Ar ambient for at least 7 days (~6×10^5 s). The thermal stability of Cu/$CN_{0.15}$/Pt is superior to that of carbon-,[23,24] oxide-,[25] or silicon-based (Ref. 14) memristive devices in which the RS originates from the

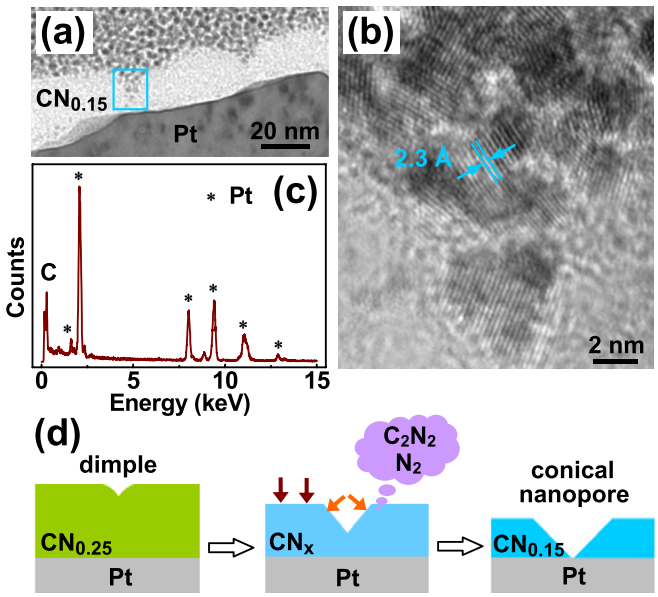

FIG. 2. (a) Cross-sectional TEM image of $CN_{0.15}$ thin films. The specimen was prepared by an FIB system. Protective layer of Pt was locally deposited on the film to prevent beam-induced damage. More importantly, Pt acts as the pore filler facilitating the TEM observation of nanopores. (b) HRTEM image for the area marked by the light blue rectangle. The lattice distance 2.3 Å corresponds to the Pt (111) plane. (c) EDX spectra for the protective layer of Pt. (d) Schematic illustration of the formation process of conical nanopores in N-doped carbon thin films. The film thickness is reduced due mainly to the reactions at the surface (see the brown arrows). The dimples on the surface are apt to evolve into conical pores (see the orange arrows). CN_x represents intermediate products, where x is in the range of 0.15~0.25.

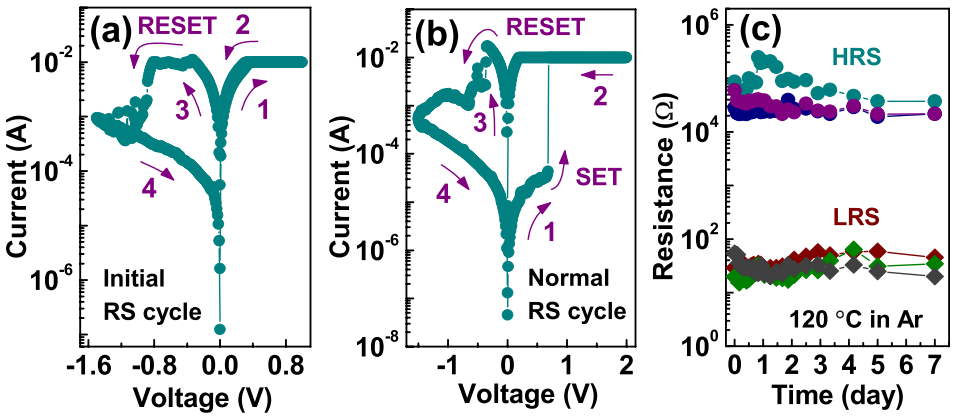

FIG. 3. (a) Initial and (b) normal *I–V* curves of Cu/$CN_{0.15}$/Pt in semilogarithmic scale. (c) Retention performance of Cu/$CN_{0.15}$/Pt at 120 °C in Ar ambient. During the retention measurement, the resistance values were read at 0.1 V.

electrically induced formation/rupture of metal (Cu, Ag, etc.) filaments. So, the Cu/$CN_{0.15}$/Pt memristive device is promising for resistance memory applications, especially for the memory devices working at elevated temperatures. The superior high temperature retention performance of Cu/$CN_{0.15}$/Pt is most likely to be attributed to (i) single-crystalline Cu filaments confined in conical nanopores which will be discussed in the following text, (ii) improved thermal stability of the carbon film by N-doping,[26] and (iii) thermal annealing of the film at 600 °C.

Figure 4(a) shows the cross-sectional TEM image of the pristine Cu/$CN_{0.15}$/Pt device. A dark zone showing a cone shape was clearly observed in the $CN_{0.15}$ layer. The energy dispersive X-ray (EDX) spectra indicate that the dark zone is composed of Cu, demonstrating that the dark zone is a Cu filament confined in a conical nanopore which should be formed during the Cu top electrode deposition process. Figures 4(b) and 4(c) present the HRTEM image of the dark zone and the corresponding image reconstructed from the filtered fast Fourier transform (FFT) image, respectively. The lattice distance is 2.06 Å corresponding to the Cu (111) plane. From Fig. 4(c), we can see that the Cu filament has a single-crystalline structure. However, the crystal lattice is not perfect, and dislocations can be found which result in obvious lattice distortions, as shown in Fig. 4(c). Figure 4(d) presents resistance versus temperature plots for Cu/$CN_{0.15}$/Pt in initial, ON, and OFF states. The resistance of the devices in initial and ON states increases linearly with temperature, demonstrating a typical metallic behavior. The temperature dependence of metallic resistance can be written as $R(T) = R_0[1 + \alpha(T - T_0)]$, where R_0 is the resistance at temperature T_0, and α is the temperature coefficient of resistance. By choosing T_0 as 300 K, the coefficient α is calculated to be 2.1×10^{-3} and $1.7 \times 10^{-3}\,K^{-1}$ for the devices in initial and ON states, respectively, which are similar to the value $2.5 \times 10^{-3}\,K^{-1}$ for high-purity Cu nanowires,[27,28] but lower than that for bulk Cu ($3.9 \times 10^{-3}\,K^{-1}$). It confirms the existence of Cu nanofilaments in the conical through-pores. It is worth noting that only the pristine Cu/$CN_{0.15}$/Pt device contains complete single-crystalline Cu filaments, since part of the filament is electrochemically dissolved during the RESET process. The following SET process electrochemically rejuvenates the previously dissolved filament segment, and the rejuvenated filament segment is most likely composed of continuous Cu nano-grains rather than a single crystal.[21] Given that the filament is apt to be ruptured at the weakest position along its length,[9,29] the rupture/rejuvenation of the Cu filaments should occur around the $CN_{0.15}$/Pt interface. From Fig. 4(d), we also see that the OFF state exhibits a tunneling behavior, since the resistance shows a weak dependence of temperature.[20] Then, the dissolved filament segment during the RESET process is only several nanometers in length. We can therefore deduce that for the device in an OFF or ON state, the Cu filaments, for the most part, keep the single-crystalline structure.

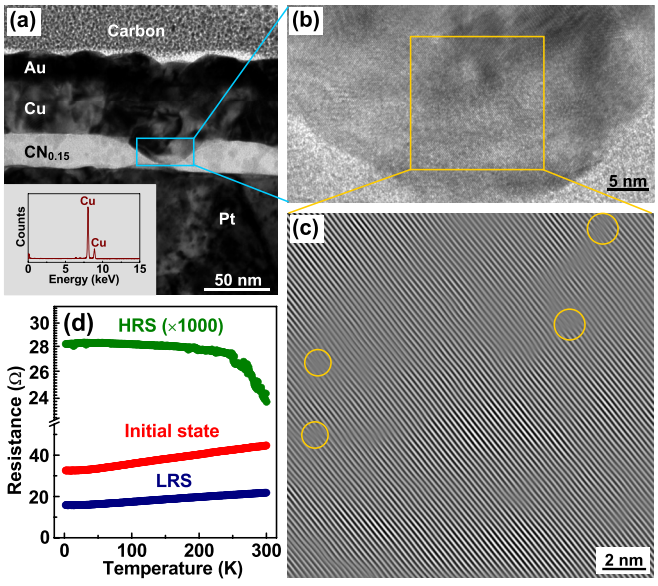

FIG. 4. (a) Cross-sectional TEM image of the pristine Cu/$CN_{0.15}$/Pt device. The specimen was prepared by an FIB system. Protective layer of carbon was locally deposited on the device to prevent beam-induced damage. The inset shows the EDX spectra for the area marked by the light blue rectangle. (b) HRTEM image for the area marked by the light blue rectangle in (a). (c) The image reconstructed from the filtered FFT image for the area marked by the yellow rectangle in (b). The yellow circles highlight the existing dislocations. (d) Resistance versus temperature plots for Cu/$CN_{0.15}$/Pt in initial, ON, and OFF states.

Figure 5(a) shows *I–V* characteristics of Cu/$CN_{0.15}$/Pt measured by a modified voltage sweep. First, a continuous RESET process was performed with a consecutive increase of the stop voltage from −0.3 to −1.3 V. Then, a continuous SET process was performed with an increase of the current compliance (CC) from 22 μA to 3.5 mA. Figure 5(b) shows a gradual increase of the device conductance by using positive voltage pulses with increasing CC from 20 μA to 2.6 mA,

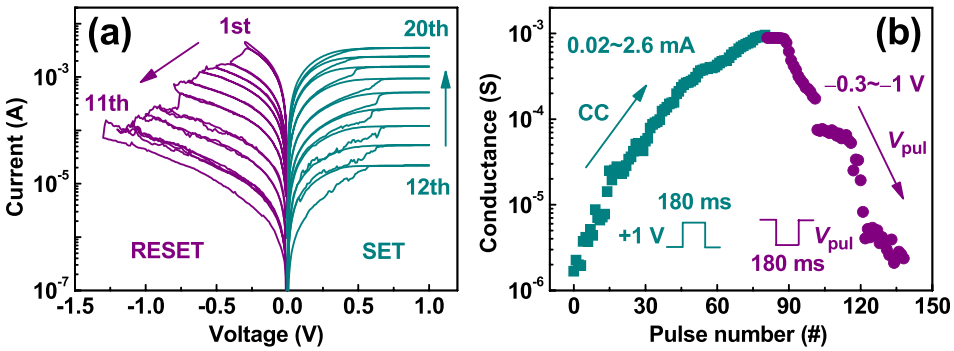

FIG. 5. (a) *I–V* characteristics of Cu/$CN_{0.15}$/Pt measured by a modified voltage sweep. (b) Gradual increase of the device conductance by using positive voltage pulses with increasing CC and gradual decrease of the conductance by using negative pulses with increasing voltage amplitude. Herein, the consecutive increase of CC was implemented by a series connected transistor.

and subsequent gradual decrease of the conductance by using negative pulses with increasing voltage amplitude from −0.3 to −1 V. The results indicate that multi-level resistance states can be obtained by varying the CC level or voltage amplitude in both voltage sweeping and pulse modes. So, the Cu/$CN_{0.15}$/Pt memristive device can potentially be used as an electronic synapse device.[30–32]

In conclusion, we have investigated the single-crystalline Cu filament-based resistive switching in Cu/$CN_{0.15}$/Pt memristor devices in which the Cu filaments are confined in conical nanopores in the $CN_{0.15}$ thin film. The device exhibits outstanding thermal stability. Thus, it is promising for resistance memory applications, especially for the memory devices working at elevated temperatures. Furthermore, continuous RESET and SET processes have been realized in Cu/$CN_{0.15}$/Pt, indicating that it can potentially be used as an electronic synaptic device.

This work was supported by National Natural Science Foundation of China (Nos. 51272261 and 61474127) and Chinese National Program on Key Basic Research Project (No. 2012CB933003).

[1]R. Waser, R. Dittmann, G. Staikov, and K. Szot, Adv. Mater. **21**, 2632 (2009).
[2]F. Pan, S. Gao, C. Chen, C. Song, and F. Zeng, Mater. Sci. Eng., R **83**, 1 (2014).
[3]I. Valov, E. Linn, S. Tappertzhofen, S. Schmelzer, J. van den Hurk, F. Lentz, and R. Waser, Nat. Commun. **4**, 1771 (2013).
[4]Y. C. Yang, P. Gao, S. Gaba, T. Chang, X. Q. Pan, and W. Lu, Nat. Commun. **3**, 732 (2012).
[5]T. Tsuruoka, K. Terabe, T. Hasegawa, and M. Aono, Nanotechnology **21**, 425205 (2010).
[6]Y. C. Yang, F. Pan, Q. Liu, M. Liu, and F. Zeng, Nano Lett. **9**, 1636 (2009).
[7]Q. Liu, J. Sun, H. B. Lv, S. B. Long, K. B. Yin, N. Wan, Y. T. Li, L. T. Sun, and M. Liu, Adv. Mater. **24**, 1844 (2012).
[8]F. Zhuge, S. S. Peng, C. L. He, X. J. Zhu, X. X. Chen, Y. W. Liu, and R. W. Li, Nanotechnology **22**, 275204 (2011).
[9]S. S. Peng, F. Zhuge, X. X. Chen, X. J. Zhu, B. L. Hu, L. Pan, B. Chen, and R. W. Li, Appl. Phys. Lett. **100**, 072101 (2012).
[10]K. Terabe, T. Hasegawa, T. Nakayama, and M. Aono, Nature **433**, 47 (2005).
[11]T. A. Miller, J. S. Wittenberg, H. Wen, S. Connor, Y. Cui, and A. M. Lindenberg, Nat. Commun. **4**, 1369 (2013).
[12]M. N. Kozicki and M. Mitkova, J. Non-Cryst. Solids **352**, 567 (2006).
[13]L. Chen, Y. D. Xia, X. F. Liang, K. B. Yin, J. Yin, and Z. G. Liu, Appl. Phys. Lett. **91**, 073511 (2007).
[14]S. Jo, K. Kim, and W. Lu, Nano Lett. **9**, 496 (2009).
[15]P. G. Peng, D. Xie, Y. Yang, Y. Y. Zang, X. L. Gao, C. J. Zhou, T. T. Feng, H. Tian, T. L. Ren, and X. Z. Zhang, J. Appl. Phys. **111**, 084501 (2012).
[16]Y. Chai, Y. Wu, K. Takei, H. Y. Chen, S. M. Yu, P. C. H. Chan, A. Javey, and H. Philip, IEEE Trans. Electron Devices **58**, 3933 (2011).
[17]F. Zhuge, W. Dai, C. L. He, A. Y. Wang, Y. W. Liu, M. Li, Y. H. Wu, P. Cui, and R. W. Li, Appl. Phys. Lett. **96**, 163505 (2010).
[18]H. Choi, M. Pyun, T. W. Kim, M. Hasan, R. Dong, J. Lee, J. B. Park, J. Yoon, D. J. Seong, T. Lee, and H. Hwang, IEEE Electron Device Lett. **30**, 302 (2009).
[19]F. Zhuge, B. L. Hu, C. L. He, X. F. Zhou, Z. P. Liu, and R. W. Li, Carbon **49**, 3796 (2011).
[20]T. Sakamoto, M. Tada, K. Okamoto, and H. Hada, IEEE Trans. Electron Devices **59**, 3574 (2012).
[21]H. T. Sun, Q. Liu, C. F. Li, S. B. Long, H. B. Lv, C. Bi, Z. Huo, L. Li, and M. Liu, Adv. Funct. Mater. **24**, 5679 (2014).
[22]H. Chen, F. Zhuge, B. Fu, J. Li, J. Wang, W. G. Wang, Q. Wang, L. Li, F. G. Li, H. L. Zhang, L. Y. Liang, H. Luo, M. Wang, J. H. Gao, H. T. Cao, H. Zhang, and Z. C. Li, Carbon **76**, 459 (2014).
[23]J. Park, M. Jo, J. Lee, S. Jung, W. Lee, S. Kim, S. Park, J. Shin, and H. Hwang, Microelectron. Eng. **88**, 935 (2011).
[24]W. Lee, J. Park, M. Son, J. Lee, S. Jung, S. Kim, S. Park, J. Shin, and H. Hwang, IEEE Electron Device Lett. **32**, 680 (2011).
[25]W. H. Guan, M. Liu, S. B. Long, Q. Liu, and W. Wang, Appl. Phys. Lett. **93**, 223506 (2008).
[26]L. H. Zhang, H. Gong, and J. P. Wang, J. Phys.: Condens. Matter **14**, 1697 (2002).
[27]A. Bid, A. Bora, and A. Raychaudhuri, Phys. Rev. B **74**, 035426 (2006).
[28]S. Gao, C. Song, C. Chen, F. Zeng, and F. Pan, J. Phys. Chem. C **116**, 17955 (2012).
[29]K. M. Kim, D. S. Jeong, and C. S. Hwang, Nanotechnology **22**, 254002 (2011).
[30]Z. Q. Wang, H. Y. Xu, X. H. Li, H. Yu, Y. C. Liu, and X. J. Zhu, Adv. Funct. Mater. **22**, 2759 (2012).
[31]S. Jo, T. Chang, I. Ebong, B. Bhadviya, P. Mazumder, and W. Lu, Nano Lett. **10**, 1297 (2010).
[32]S. Yu, Y. Wu, R. Jeyasingh, D. Kuzum, and H. S. P. Wong, IEEE Trans. Electron Devices **58**, 2729 (2011).